



Published in final edited form as:

*J Immunol.* 2009 November 1; 183(9): 5738–5747. doi:10.4049/jimmunol.0901563.

## RANKL is necessary and sufficient to initiate development of antigen-sampling M cells in the intestinal epithelium

Kathryn A. Knoop<sup>\*</sup>, Nachiket Kumar<sup>\*</sup>, Betsy R. Butler<sup>\*</sup>, Senthilkumar K. Sakthivel<sup>\*</sup>, Rebekah T. Taylor<sup>\*</sup>, Tomonori Nochi<sup>†</sup>, Hisaya Akiba<sup>‡</sup>, Hideo Yagita<sup>‡</sup>, Hiroshi Kiyono<sup>†</sup>, and Ifor R. Williams<sup>\*</sup>

<sup>\*</sup>Department of Pathology and Laboratory Medicine, Emory University School of Medicine, Atlanta, GA 30322

<sup>†</sup>Division of Mucosal Immunology, Department of Microbiology and Immunology, University of Tokyo, Tokyo, Japan

<sup>‡</sup>Department of Immunology, Juntendo University School of Medicine, Tokyo, Japan

### Abstract

Microfold cells (M cells) are specialized epithelial cells situated over Peyer's patches (PP) and other organized mucosal lymphoid tissues that transport commensal bacteria and other particulate antigens into intraepithelial pockets accessed by antigen-presenting cells. The TNF superfamily member RANKL is selectively expressed by subepithelial stromal cells in PP domes. We found that RANKL null mice have less than 2% of wild type levels of PP M cells and markedly diminished uptake of 200 nm diameter fluorescent beads. Antibody-mediated neutralization of RANKL in adult wild type mice also eliminated most PP M cells. The M cell deficit in RANKL null mice was corrected by systemic administration of exogenous RANKL. Treatment with RANKL also induced the differentiation of villous M cells on all small intestinal villi with the capacity for avid uptake of *Salmonella* and *Yersinia* organisms and fluorescent beads. The RANK receptor for RANKL is expressed by epithelial cells throughout the small intestine. We conclude that availability of RANKL is the critical factor controlling the differentiation of M cells from RANK-expressing intestinal epithelial precursor cells.

### Introduction

The organized lymphoid tissues of the intestine are inductive sites for both the generation of secretory IgA and the generation of T cell tolerance to antigens present in the intestinal lumen, including those derived from food and the commensal flora (1,2). The follicle-associated epithelium (FAE) that covers the lymphoid follicles of both Peyer's patches (PP) and isolated lymphoid follicles (ILF) contains specialized epithelial cells known as microfold cells (M cells) that provide a portal for efficient sampling of particulate antigens from the lumen (3,4). Antigens acquired through this major pathway for antigen sampling in the intestine are delivered into intraepithelial pockets within the M cells that lymphocytes and APC access from the subepithelial dome region. The M cell-mediated antigen-sampling pathway has a central role in the development of immune responses to both pathogenic bacteria and commensal bacteria. Production of protective fecal IgA in mice after oral infection with invasive *Salmonella* species requires the presence of PP with M cells (5,6). In

<sup>2</sup>Address correspondence and reprint requests to Dr. Ifor R. Williams, Department of Pathology and Laboratory Medicine, Emory University School of Medicine, Whitehead Bldg. 105D, 615 Michael St., Atlanta, GA 30322, Phone: 404-727-8547, Fax: 404-727-8538, irwilli@emory.edu.

addition, some commensal bacteria internalized through M cells are passed into dendritic cells that travel with their cargo to the draining mesenteric lymph node, leading to both IgA antibody production and establishment of T cell tolerance (7). M cells also promote the development of T cell tolerance to antigens acquired through the gastrointestinal tract. Targeting OVA to mouse M cells via the reovirus sigma 1 protein resulted in enhanced development of oral tolerance in CD4<sup>+</sup> T cells (8). While most M cells in the small intestine of wild type mice are localized to the FAE of PP and ILF, occasional villi contain clusters of cells known as villous M cells that exhibit all the major defining characteristics of PP M cells including reactivity with the *Ulex europaeus* agglutinin-I (UEA-I) lectin recognizing  $\alpha(1,2)$ -fucose, stubby microvilli, and the capacity to ingest and transcytose particles the size of bacteria (9).

While the basic functional and ultrastructural features of M cells were initially described over 30 years ago (10), many basic questions about M cell differentiation and function remain unsolved. It has been proposed that specific factors released from the lymphoid microenvironment immediately beneath the FAE have the potential to elicit M cell differentiation in the FAE and promote the function of M cells, but specific signaling mediators with such activity have not been identified to date (11,12). Debate continues on whether M cells are a distinct lineage arising from crypt stem cells like other differentiated intestinal epithelial cells or whether M cells can instead arise from normal FAE enterocytes with the plasticity to transition into M cells upon encountering the right set of stimuli (13–15).

RANKL (receptor activator of NF- $\kappa$ B ligand) is a member of the TNF superfamily (16) that is also referred to as TNF-related activation-induced cytokine and TNFSF11. Like TNF- $\alpha$ , RANKL is initially synthesized as a transmembrane protein that can be released from the cell surface following cleavage by one of several metalloproteases (17,18). RANKL signals through its receptor RANK (receptor activator of NF- $\kappa$ B) and a downstream pathway that involves TRAF6 and the activation of NF- $\kappa$ B (19,20). Osteoprotegerin (OPG) is a soluble decoy receptor for RANKL that allows for tight regulation of the circulating levels of RANKL (21). A major breakthrough in establishing a biological role for RANKL-RANK interactions was the discovery that RANKL signaling through RANK is required for normal osteoclast function (22,23). Mice deficient in either RANKL or RANK have osteopetrosis and severe skeletal abnormalities because they lack the number of osteoclasts needed to remodel bone normally. RANKL-RANK signaling is also involved in several other critical biological processes including development of lymph nodes, development of medullary thymic epithelial cells (mTEC), mammary gland lactation, and provision of survival signals to dendritic cells (22–27). The absence of all lymph nodes in RANKL-deficient mice demonstrates that RANKL is an essential mediator in lymphoid organogenesis (22,23). RANKL induces lymphotoxin (LT)  $\alpha_1\beta_2$  expression by lymphoid tissue inducer cells in the lymph node anlage (28). RANKL is not required for PP development, but the reduced size of PP reported in two independent lines of RANKL-deficient mice indicates that RANKL contributes to normal PP development (22,23). Functional studies of PP were not done as part of the initial characterization of these mice.

We previously showed that RANKL is selectively expressed by stromal cells in the subepithelial dome region beneath the FAE of both PP and ILF (29). Stromal cells with phenotypic characteristics similar to neonatal lymph node organizer cells including RANKL expression were recently identified in multiple secondary lymphoid tissues including mucosal-associated lymphoid tissues and lymph nodes (30). The polarized pattern of RANKL expression by stromal cells beneath the FAE of PP and ILF suggested a possible function for RANKL in regulating the induction of mucosal immune responses to particulate luminal antigens taken up through the FAE. In this study, we evaluated the function of PP in

RANKL null mice and found that absence of RANKL is associated with loss of the vast majority of UEA-I<sup>+</sup> M cells in the FAE. The depletion of M cells correlated with a profound functional defect in uptake from the intestinal lumen of fluorescent beads used as model particulate antigens. Systemic administration of exogenous soluble RANKL restored functional UEA-I<sup>+</sup> M cells to the PP of RANKL null mice and simultaneously led to widespread induction of functional M cells on the epithelium covering small intestinal villi in both RANKL null mice and wild type mice. These findings demonstrate that the RANKL-RANK pathway plays a pivotal nonredundant role in establishing the M cell-mediated pathway of antigen acquisition and handling.

## Materials and Methods

### Mice

Mice carrying a RANKL null mutation on a C57BL/6 background (31) obtained from Dr. Yongwon Choi at the University of Pennsylvania (Philadelphia, PA) were used to establish a breeding colony in a conventional specific pathogen free mouse facility at Emory University. Serological sentinel testing in this facility did not include routine testing for *Helicobacter* or *Pasteurella* species, but no infections attributed to these opportunistic pathogens were demonstrated in the colony of RANKL null mice or their controls. Because RANKL null mice lack teeth, weanling null mice born in this colony are routinely given powdered mouse chow. Mice heterozygous for the RANKL null mutation were also backcrossed to BALB/c mice (Taconic) for a total of 4 generations. Male C57BL/6 RANKL<sup>+/-</sup> mice and female BALB/c RANKL<sup>+/-</sup> mice were intercrossed to produce RANKL null mice and littermate controls on a background roughly equivalent to (C57BL/6 X BALB/c)F<sub>1</sub> mice. RANKL null mice on this “F1 equivalent” genetic background are closer in weight to their heterozygous and wild type littermates and less likely to die prematurely compared to RANKL null mice on the two inbred backgrounds. Experiments using RANKL null mice were done with mice on a C57BL/6 background mice, a (C57BL/6 X BALB/c)F<sub>1</sub> background, or a mixed C57BL/6 and BALB/c background, as indicated in the figure legends. BALB/c mice (Taconic) were used for experiments examining induction of villous M cells by RANKL in wild type mice and the effects of anti-RANKL mAb on PP M cells. All animal studies were reviewed and approved by the Emory University Institutional Animal Care and Use Committee.

### Recombinant mouse RANKL

A bacterial expression construct encoding a glutathione S-transferase (GST) fusion protein containing amino acids 137–316 of mouse RANKL was assembled in the pGEX-5X-1 vector (GE Healthcare) using a modification of a previously described method (32). The primers 5'-CACCCCCGGGTCAGCGCTTCTCAGGAGCT-3' and 5'-CTCGAGTCAGTCTATGTCCTGAAC-3' were used to PCR amplify a cDNA clone for mouse RANKL (Open Biosystems). After the PCR product was cloned into the pENTR-D-TOPO cloning vector (Invitrogen) and sequenced, the SmaI-XhoI fragment was subcloned into pGEX-5X-1. The construct was transformed into the BL21 *E. coli* strain (Stratagene) for fusion protein expression. The cultures were induced with 20 μM IPTG for 16 hours at 20°C and the GST-RANKL purified from bacterial lysate by affinity chromatography on a GSTrap FF column (GE Healthcare) followed by dialysis against multiple changes of PBS. Recombinant GST used as a control was prepared by the same method using empty pGEX-5X-1. Biological activity of the GST-RANKL fusion protein was confirmed by its ability to induce differentiation of the RAW264.7 macrophage line (American Type Culture Collection) into multinucleate osteoclasts positive for tartrate resistant acid phosphatase. The GST-RANKL fusion protein was administered to RANKL null mice by daily i.p. or s.c.

injections of 50 to 250  $\mu\text{g}$  per day for up to 7 days. Recombinant GST prepared from empty pGEX-5X-1 vector was used as a control for GST-RANKL.

### Bacterial strains

A wild type strain of *Salmonella enterica* serovar Typhimurium (SL3201) transformed with the DsRed-Express plasmid (Clontech) encoding a cytoplasmic red fluorescent protein was kindly provided by Dr. Andrew Neish at Emory University. A *Yersinia enterocolitica* isolate (ATCC 29913) was purchased from the ATCC (Manassas, VA). For experiments involving injection of bacteria into isolated intestinal loops, these bacteria were grown overnight in LB broth, washed in PBS, and fixed in 2% paraformaldehyde for 1 h. The fixed *Yersinia* were then labeled with Alexa546-succidymyl ester (Molecular Probes) for 1 h at room temperature following the manufacturer's suggestions.

### In vivo assessment of M cell uptake of fluorescent beads and bacteria

The uptake of 200 nm diameter fluorescent polystyrene latex nanoparticles (Fluoresbrite YG; Polysciences) and fluorescent bacteria by M cells in the FAE of individual PP or by villous M cells induced by exogenous RANKL treatment was assessed by either oral gavage or by using a modification of previously described isolated small intestinal loop models (33,34). In oral gavage experiments examining uptake of the by RANKL-induced villous M cells, aliquots of  $1 \times 10^{11}$  200 nm diameter nanoparticles in a volume of 200  $\mu\text{l}$  were fed to the mice. To prepare isolated small intestinal loops, mice were anesthetized using an isoflurane vaporizer. After opening the peritoneum through a longitudinal midline incision, 2 or 3 segments of small intestine measuring 2–5 cm in length and containing either a single PP (to assess PP M cell uptake) or no PP (to assess villous M cell uptake) were tied off with nylon filament. For bead uptake studies, the loops were injected with 200–400  $\mu\text{l}$  of a suspension of 200 nm nanoparticles diluted in PBS to a concentration of  $1 \times 10^{11}$  beads/ml and returned to the peritoneal cavity. The mice were euthanized 90 to 120 minutes after the loops were injected, and the injected intestinal segments were excised, washed in 0.5% Tween 20-PBS, fixed in 4% paraformaldehyde in PBS for 15 minutes, and embedded in OCT. Frozen sections cut from these intestinal segments were examined by microscopy after counterstaining with 4',6-diamidino-2-phenylindole (DAPI), leaving out a cold acetone fixation step because acetone dissolved the polystyrene Fluoresbrite beads, preventing their visualization. For bacterial uptake studies, loops containing no PP were injected with 300 to 500  $\mu\text{l}$  of bacterial suspension at a concentration of  $5 \times 10^9$  organisms/ml. After 120 minutes the mice were euthanized and the intestine tissue within the loop was embedded in OCT as a Swiss roll. Frozen sections from this tissue were fixed with  $-20^\circ\text{C}$  acetone since this fixation did not interfere with detection of the fluorescent bacteria.

### Antibodies and lectins

Monoclonal antibodies for staining were purchased from eBioscience, unless otherwise stated. The mAbs used for immunofluorescence staining of frozen sections were anti-RANKL (IK22-5), anti-RANK (LOB14-8; GeneTex), PE-conjugated anti-B220 (RA3-6B2), biotinylated GL7 (for detection of activated germinal center B cells), and allophycocyanin-conjugated anti-Thy1.2 (53-2.1; BD Biosciences). The rat mAb NKM 16-2-4 specific for mouse M cells was purified from hybridoma supernatant and labeled with FITC (35). A purified rat IgG2a isotype control mAb (BD Biosciences) was used as a control for staining of frozen tissue sections with the rat IgG2a anti-RANKL and anti-RANK mAbs. Biotinylated polyclonal goat anti-rat IgG (BD Biosciences) was used as a secondary reagent for detection of most unconjugated rat primary mAb. Rhodamine-UEA-I was purchased from Vector Labs. The anti-RANKL antibody (IK22-5) used for in vivo RANKL neutralization experiments was prepared as described previously (36). Mice were treated

with 250 µg of IK22-5 or a purified functional grade control rat IgG2a mAb (eBioscience) i.p. every 2 days.

### Immunofluorescence staining of frozen sections

Frozen sections of PP and adjacent intestinal tissue were cut on a cryostat and prepared for antibody staining experiments as previously described (29). The sections were washed in PBS and blocked in TNB buffer (PerkinElmer Life Sciences). Antibodies diluted in TNB buffer were applied for one hour at room temperature or overnight at 4°C. Biotinylated primary mAbs were detected using streptavidin-conjugated peroxidase followed by FITC-tyramide from a tyramide signal amplification kit (PerkinElmer Life Sciences). Unconjugated primary rat mAbs were detected by a combination of biotinylated polyclonal goat-anti-rat IgG (BD Biosciences) followed by streptavidin-peroxidase and FITC-tyramide. DAPI (Sigma-Aldrich) at 10 ng/ml was used as a nuclear counterstain. The slides were mounted in ProLong antifade reagent (Invitrogen). Images were acquired using a Nikon 80i fluorescence microscope and edited when necessary with Photoshop (Adobe Systems).

### Electron microscopy

Mice were perfusion fixed using 2.5% glutaraldehyde solution in 0.1M cacodylate buffer. For transmission electron microscopy, individual PP were isolated, bisected through the center of the domes, and embedded in Epon resin. Thin sections from the PP domes of control and RANKL null mice were examined using a JEOL JEM-1210 microscope. For scanning electron microscopy, small intestinal villi were subjected to critical point drying, sputter coated with gold, and examined on a Topcon DS-130F field emission scanning electron microscope.

### Whole mount staining of small intestine tissue for detection of UEA-I<sup>+</sup> M cells

For detection of M cells in PP, individual PP were excised and vortex mixed in 0.5% Tween20-PBS followed by a shaking incubation with 100 µg/ml DNase for 20 minutes at 37°C to promote dissociation of mucus from the epithelial layer. The PP were blocked with TNB buffer for 15 minutes at 4°C, and stained with rhodamine-UEA-I in TNB for 40 minutes at 4°C. Each stained PP was mounted under a 20 mm X 20 mm coverslip in 100 µl PBS. A count of UEA-I<sup>+</sup> M cells was done for the PP follicle with the most M cells. This method resulted in some degree of underestimation of the full extent of M cell depletion in RANKL null mice because often only one of several PP follicles had any M cells in the mutant mice, while all the follicles in wild type PP typically had a comparable number of M cells. To examine small intestine tissue for the presence of villous M cells, thin strips of tissue were cut and stained with rhodamine UEA-I as described above for PP. Villi with M cells on their surface were classified as showing a dense or diffuse pattern of villous M cells using criteria based on the initial description of these patterns by Jang et al. (9). Specifically, villi with one or more clusters of M cells in which 75% or more of the area within the cluster was occupied with M cells were considered to have a dense distribution of villous M cells. Villi with at least one characteristic UEA-I<sup>+</sup> M cell on the surface, but not meeting the dense distribution criteria, were considered to have a diffuse distribution.

### Quantitative analysis of fluorescent bead and bacteria uptake by M cells

Analysis of the degree of bead uptake from loops containing PP was done by threshold analysis using ImageJ v1.36b software (<http://rsb.info.nih.gov/ij/>). Images of the fluorescent beads found within sections of individual PP follicles were saved as 8-bit grayscale images and then converted to binary images showing the beads by thresholding at a grayscale cutoff point of 75 out of 255. The percentage of the pixels with a signal intensity that exceeded this cutoff was calculated for the area occupied by each PP follicle. Analysis of the bead uptake



from loops lacking PP was done by a similar approach. Images of sections showing just the fluorescent beads within epithelial cells and the villi were thresholded at a grayscale cutoff point of 55 out of 255. Images of the DAPI-stained nuclei in the same field acquired in a separate channel were thresholded at a cutoff point of 70. The extent of bead uptake was expressed as the ratio of pixels with fluorescent beads to pixels with DAPI after normalization to a mean value of 1.0 for loops from mice not treated with RANKL. Analysis of fluorescent bacteria uptake from loops lacking PP was done by counting of the number of organisms present in sections of villi showing the villus from its base to the tip. The data were reported as the percentage of villi that included at least one organism and the average number of organisms per villus. The latter statistic was normalized to a value of 1.0 for loops from mice not treated with RANKL.

### ELISA for measurement of fecal IgA

Fecal pellet samples were collected and extracted by making a 1:10 suspension (w/v) with PBS. After the suspension was vortexed and spun for 10 min at 12,000g, the supernatant was stored at  $-70^{\circ}\text{C}$ . Polyclonal goat anti-mouse IgA antibody (Southern Biotechnology) was used as a capture antibody. The bound mouse IgA was detected with peroxidase-labeled goat anti-mouse IgA antibody (Southern Biotechnology) using TMB (BD Biosciences) as the peroxidase substrate. A mouse IgA, $\kappa$  isotype control mAb (BD Biosciences) was used to establish a standard curve.

### Statistical analysis

Differences between the mean values for groups were analyzed by either two-tailed ANOVA with Tukey correction (for multiple groups), two-tailed Student's *t* test, or two-tailed Mann-Whitney test as calculated using Prism (GraphPad Software). Differences in the frequency of bacterial uptake into villi were analyzed by Fisher's exact test and also calculated with Prism. A *p* value of less than 0.01 was considered significant.

## Results

### UEA-I<sup>+</sup> M cells are dramatically decreased in the FAE of PP from RANKL null mice

M cells in mouse PP can be detected using the UEA-I lectin specific for  $\alpha(1,2)$ -fucose linkages. In wild type mice, whole mount microscopy of PP follicles revealed an average of over 100 radially arranged UEA-I<sup>+</sup> M cells that extended from the edges of the follicles towards the central subepithelial dome area. In contrast, UEA-I<sup>+</sup> M cells were either completely absent or very sparsely represented in individual follicles from the PP RANKL null mice (Fig. 1A). The few remaining UEA-I<sup>+</sup> cells in RANKL null mice were mostly located at the periphery of the follicle and did not have the usual polygonal shape of normal M cells, features suggesting these remaining M cells were abnormal. The loss of M cells in PP from RANKL null mice was confirmed by staining PP sections with NKM 16-2-4 (Fig. S1), a recently described rat mAb that is more selective than UEA-I for the specific  $\alpha(1,2)$ -fucose moiety characteristically displayed by mouse M cells (35). Cells with the defining ultrastructural features of M cells by transmission electron microscopy (i.e. presence of intraepithelial pockets and blunting of the apical microvilli in comparison to normal enterocytes) were readily apparent in the FAE from control mice, but absent from the FAE of RANKL null mice (Fig. 1B). While the number of UEA-I<sup>+</sup> M cells was significantly decreased in all PP examined from RANKL null mice, a proximal to distal gradient in the number of UEA-I<sup>+</sup> cells per dome was observed in RANKL null mice that was not seen in wild type mice (Fig. 1C). UEA-I<sup>+</sup> M cells were almost completely absent in the most proximal PP from RANKL null mice, and progressively increased in more distal PP. In RANKL null mice, the highest number of residual UEA-I<sup>+</sup> cells was consistently detected in the most distal ileal PP. Taking into account the decreases in RANKL null mice in the

number of PP, the number of follicles in each PP, and the number of M cells per follicle, loss of RANKL is associated with a 73-fold overall depletion of UEA-I<sup>+</sup> M cells. This extent of loss of M cells is roughly 10-fold greater than the losses we observed in both  $\mu$ MT B cell deficient mice and CCR6 deficient mice (data not shown), strains of mutant mice previously shown to have a significant reduction in the number of M cells (37,38).

### **UEA-I<sup>+</sup> M cells can be restored in RANKL null mice by treatment with exogenous RANKL**

To determine if the deficiency of M cells in the FAE of RANKL null PP could be restored by replacement of RANKL, RANKL null mice were injected i.p. for 7 consecutive days with 250  $\mu$ g per day of either recombinant GST-RANKL fusion protein or recombinant GST as a control. On day 7, the PP follicles of RANKL null mice treated with GST-RANKL had a near normal number of UEA-I<sup>+</sup> M cells distributed in the typical radial pattern, while GST-treated mice remained profoundly M cell deficient (Fig. 2A). Daily treatment of RANKL null mice with rGST-RANKL for shorter intervals demonstrated that day 5 was the first time point at which the number of UEA-I<sup>+</sup> M cells was significantly increased over untreated RANKL null mice (Fig. 2B).

### **RANKL null mice have a defect in the uptake of 200 nm fluorescent beads into PP follicles that is corrected by administration of RANKL**

While UEA-I is a useful immunohistochemical marker of mouse M cells, this method of identification does not detect M cells based on their specialized ability to take up particulate antigens from the lumen and transport them to meet APC in the intraepithelial pockets. Measuring uptake of fluorescent nanoparticles injected into loops of small intestine is a method that directly assesses M cell function in the FAE of PP (33,34). Frozen sections of PP in isolated loops of small intestine from RANKL null mice and RANKL null mice treated with GST-RANKL or GST (as a control) were compared at 90 minutes after injection of fluorescent 200 nm nanoparticles into the loops. In the GST-RANKL-treated mice more UEA-I<sup>+</sup> M cells were present and some of these cells contained multiple fluorescent beads (Fig. 2C). Beads that had already passed through the epithelial layer to reach the PP follicle were observed in APC in the vicinity of the subepithelial dome or deeper in the B cell follicle. Image analysis was used to quantify the magnitude of bead uptake in the GST-RANKL reconstituted mice and controls (Fig. 2D). Untreated RANKL null mice or those treated with GST had over 10-fold less uptake of beads than control wild type mice. GST-RANKL treatment for 7 days restored bead uptake to near wild type levels.

### **Systemic administration of RANKL also leads to widespread induction of villous M cells**

In the course of treating RANKL null mice with GST-RANKL and evaluating the reconstitution of M cells in PP, we noticed that the number of UEA-I<sup>+</sup> cells present on small intestinal villi was also increased. This effect of RANKL treatment was further evaluated in BALB/c mice, in which less than 10% of small intestinal villi have any villous M cells at baseline, with most of these rare villous M cells arranged in a diffuse pattern. Treatment with systemic GST-RANKL i.p. for 4 consecutive days induced substantial increase in the number of UEA-I<sup>+</sup> cells with the features of M cells on the surface of the villi (Fig. 3A). Induction of an increased number of villous M cells began by 24 hours after the first injection of GST-RANKL; 4 days after the start of RANKL treatment all small intestinal villi had at least some UEA-I<sup>+</sup> cells present, with 70% of villi showing a diffuse pattern and the remaining 30% exhibiting a dense pattern (Fig. 3B). In villi showing a diffuse pattern of villous M cells, UEA-I<sup>+</sup> cells represented approximately 3% of the total number of cells with DAPI<sup>+</sup> nuclei. Scanning electron microscopy of villi from RANKL-treated mice revealed slightly sunken cells with the characteristic stubby microvilli characteristic of M cells (Fig. 3C).

### **RANKL-induced villous M cells are functional M cells capable of taking up 200 nm beads and enteric bacteria**

To determine whether the villous M cells induced by systemic RANKL treatment were capable of increased transport of particulate antigens across the epithelium, mice were treated with s.c. injections of GST-RANKL or GST as a control for 4 consecutive days and gavaged with 200 nm diameter fluorescent nanoparticles at the same time as the last 2 RANKL injections. Small intestinal segments from these mice were excised 24 hours after the second dose of beads and frozen sections cut to identify beads that had been taken up into the lamina propria by M cells. Bead uptake was readily apparent in M cells and within the villi of the RANKL-treated mice, but barely evident in the control untreated mice (Fig. 4A). Uptake of fluorescent beads was increased by an average of 74-fold over the baseline of untreated mice as a result of RANKL-induction of villous M cells (Fig. 4B). To test whether the RANKL-induced villous M cells were also capable of enhanced uptake of enteric bacteria, isolated segments of small intestine lacking any PP from mice treated with GST-RANKL or GST for 4 days were injected with fluorescently labeled paraformaldehyde-fixed enteric bacteria. Sections of the intestinal wall taken 2 hours after the introduction of the bacteria revealed substantially enhanced uptake of both *Salmonella enterica* serovar Typhimurium (35-fold) and *Yersinia enterocolitica* (46-fold) as a consequence of villous M cell induction by RANKL (Fig. 4C and 4D).

### **Neutralizing antibody to RANKL reproduces the M cell deficiency observed in RANKL null mice**

Some of the developmental defects in RANKL null mice, such as the total absence of lymph nodes, cannot be corrected by simply injecting the mice with the absent cytokine as adults. This raises the issue of whether the M cell deficit observed in PP from RANKL null mice might be a byproduct of early developmental alterations in the PP of these mice. To address this issue, wild type BALB/c mice were treated i.p. with a neutralizing anti-RANKL antibody to determine if acute blockade of RANKL-RANK signaling would lead to loss of PP M cells. Mice were treated i.p. with 250 µg of the IK22-5 rat anti-mouse RANKL mAb every 2 days, a dose previously shown to block the activity of RANKL in vivo (36). The number of M cells in the PP follicles was evaluated after various lengths of treatment by both UEA-I staining and by uptake of fluorescent 200 nm beads from isolated small intestinal loops. After 8 days of antibody treatment, the number of M cells present in the PP and the degree of uptake of fluorescent beads by PP in isolated loops were both dramatically decreased compared to untreated mice or mice treated with an isotype control IgG2a mAb (Fig. 5A–C). Analysis of the kinetics of the anti-RANKL effects showed that the number of UEA-I<sup>+</sup> M cells dropped precipitously between 2 and 4 days, and declined further between 4 and 8 days (Fig. 5D).

### **Epithelial cells in the small intestine express RANK**

RANK is expressed by multiple cell types including osteoclasts, dendritic cells, mammary epithelial cells, and thymic epithelial cells. Since our experiments with RANKL null mice and neutralizing anti-RANKL antibody showed that RANKL is essential for normal M cell development within the FAE, we used immunohistochemical staining with anti-RANK antibodies to determine what cells in the vicinity of PP expressed the RANK. Staining for RANK was observed on the apical and basolateral aspects of epithelial cells in the FAE, and was also detected on villous and crypt epithelial cells (Fig. 6). Serial sections of the same PP showed that RANKL expression was restricted to stromal cells concentrated beneath the FAE as previously shown (29). These results suggest that RANKL exerts its effects on M cell differentiation through short-range delivery from the stromal cells to the FAE on the other side of the basement membrane.



## RANKL null mice exhibit decreased PP germinal center formation and fecal IgA production

PP were previously reported to be smaller than normal in two independently derived strains of RANKL null mice (22,23), but other aspects of PP function were not examined in the initial reports. We asked whether the loss of M cell function in RANKL null mice was associated with impaired B cell responses to antigens internalized from the intestinal lumen. We compared the frequency and extent of germinal center development in PP from RANKL null mice and littermate controls using an antibody (GL7) that preferentially binds activated germinal center B cells. Compared to PP from controls, PP from RANKL null mice at 10 to 12 weeks of age exhibited a smaller percentage of germinal centers containing GL7<sup>+</sup> cells in the B cell zones and a relative expansion of the T cell zones (Fig. 7A). This finding suggested that the production of secretory IgA might also be impaired in RANKL null mice. Fecal IgA concentrations in mice from 4 to 12 weeks of age were consistently decreased in RANKL null mice compared to littermate controls (Fig. 7B).

## Discussion

Antigen-sampling M cells have been described in both mammalian and avian species as part of the FAE covering the organized lymphoid structures of the respiratory and digestive tract (3,39,40). However, the specific signals and signaling pathways that trigger the differentiation of these M cells from precursor cells located in the stem cell zone of the crypts or from the enterocytes on the surface of the FAE remain to be identified (12). Some clues have emerged from analysis of strains of mutant mice created by gene-targeting that retain PP but exhibit decreased numbers of M cells in these PP. Specifically, B cell deficient mice such as  $\mu$ MT mice exhibit significantly reduced numbers of M cells in PP (37). Additional support for a role of B cells in promoting M cell development has come from in vitro studies in which co-culture of freshly isolated B lymphocyte or B lymphocyte lines with model intestinal epithelial cell lines cultured on semipermeable supports promoted the development of M cell-like features by the epithelial cells, including transcytosis of particulate antigens (11,41). However, neither in vivo analysis of PP from B cell deficient mice or experiments based on the in vitro M cell differentiation system have elucidated a specific mechanism by which B cells promote differentiation of M cells in the FAE.

RANKL emerged as a cytokine with a potential role in the differentiation of the FAE and M cells as a result of experiments demonstrating RANKL expression on stromal cells located immediately beneath the FAE in ILF and PP (29). To determine if PP were functionally compromised in the absence of RANKL, we characterized the PP of RANKL null mice. Staining of PP from RANKL null mice with the UEA-I lectin reactive with murine M cells revealed a profound depletion in UEA-I<sup>+</sup> cells compared to wild type mice. Taking into account all of the factors that contribute to the total number of M cells within small intestinal PP (i.e. number of PP, number of follicles per PP, number of M cells per follicle), we found that RANKL null mice have <2% of the number of UEA-I<sup>+</sup> M cells found in wild type mice. Although the UEA-I lectin was the primary immunohistochemical reagent we used to establish that RANKL null mice are deficient in M cells, we have used several independent means of confirming this deficiency in M cells including functional measurements of M cell activity using uptake of fluorescent nanoparticles and bacteria, transmission electron microscopy, and immunostaining with the NKM 16-2-4 monoclonal antibody specific for mouse M cells.

RANKL acting through its specific receptor (RANK) plays an important developmental role in multiple tissues. The most striking and best-studied of the deficits in RANKL null mice are the absence of any lymph nodes and the failure of osteoclast development, leading to osteopetrosis and a malformed skeleton. One potential explanation of the loss of M cells we observed in PP from RANKL null mice is an early developmental defect in PP development

that permanently compromises the capacity of the FAE to generate conventional M cells. Two types of experiments were done to test this possibility. First, we examined whether the M cell defect was reversible if a source of exogenous recombinant RANKL was provided. Daily injections of GST-RANKL given for 5 or more days provided a nearly complete reconstitution of the number of M cells per PP follicle. Second, we used neutralizing mAb to RANKL to test whether acute depletion of RANKL in adult wild type mice would also cause loss of M cells. After 4 days of anti-RANKL treatment to inhibit normal RANKL-RANK interactions, the number of UEA-I<sup>+</sup> M cells in each PP follicle plunged to levels approaching those in the RANKL null mice. Thus, production of RANKL must be sustained in the adult PP to permit the continued production and/or survival of M cells.

RANK is expressed on multiple cell types including osteoclasts and their precursors, dendritic cells, endothelial cells, mTEC, and mammary epithelial cells. The simplest model to explain the observed effects of RANKL on M cell differentiation is to propose that RANKL derived from the subepithelial dome stromal cells in the PP acts in a paracrine fashion on the adjacent epithelial cells of the FAE. Because RANKL is a type II membrane protein that is synthesized in a transmembrane form, cleavage by metalloproteases is needed to generate a soluble form of the cytokine (17,18). We favor the hypothesis that RANKL is acting directly through RANK on enterocytes because immunohistochemical staining of small intestinal tissue including a PP showed that the bulk of the RANK staining is localized to the epithelium, with roughly equivalent levels of RANK on the FAE and villous epithelium. Gene expression profiling studies comparing flow sorted PP M cells and villous enterocytes revealed that both of these intestinal epithelial cell types express mRNA for RANK (35) (gene expression data for RANK archived in NCBI Gene Expression Omnibus under accession number GSE7838; <http://www.ncbi.nlm.nih.gov/geo/query/acc.cgi?acc=GSE7838>). While the induction of M cells by RANKL appears to be mediated by direct action of RANKL on RANK-expressing epithelial cells, other cell types in the small intestine are known to express RANK and respond to RANKL. For example, RANKL was shown to act on PP DC to enhance IL-10 production (42). In addition, antibody-mediated neutralization of RANKL in a transfer model of colitis resulted in decreased regulatory T cell activity, suggesting that RANKL-RANK signaling contributes to the normal function of regulatory T cells (43).

The capacity of soluble recombinant RANKL injected systemically to induce the appearance of M cells on all small intestinal villi provides further insights into the mechanism of action of RANKL. RANK-expressing epithelial precursor cells located in both dome-associated crypts next to PP follicles and in standard small intestinal crypts have the potential to differentiate into M cells if exposed to sufficient stimulation with RANKL. RANKL-induced villous M cells have most of the same features as PP M cells, including reactivity with UEA-I, stubby surface microvilli observed by scanning electron microscopy, and most importantly the capacity for constitutive uptake of particulate antigens. Under normal conditions, M cell development is primarily restricted (other than a small number of scattered villous M cells) to the organized lymphoid tissues of the small intestine (i.e. PP and ILF) because constitutive expression of RANKL is restricted to subepithelial stromal cells at these sites. When the spatial restriction of RANKL availability in the small intestine is bypassed by systemic injection, RANKL is able to trigger M cell differentiation in a fraction of epithelial precursors in both dome-associated crypts adjacent to organized lymphoid tissues and normal crypts.

While our results identify RANKL as a key cytokine signal involved in inducing the differentiation of M cells from precursors in the FAE, we consistently observed a trace number of residual UEA-I<sup>+</sup> M cells in a few of the PP follicles in RANKL null mice. Our results fit best with a model that postulates that there are additional signals besides RANKL

that contribute to the development of M cells. We found that the most distal PP in RANKL null mice was invariably the PP with the largest number of residual M cells per follicle, suggesting that an increased density of luminal commensal bacteria can accentuate the extent of M cell differentiation locally in situations in which loss of an M cell-inducing factor results in a global decrease in M cell differentiation. One of the other signals capable of promoting M cell development may be contributed by local B cells in the PP, since absence of mature B cells also leads to depletion of PP M cells (37), although the degree of M cell deficit is far less pronounced. Exogenous administration of GST-RANKL to B cell deficient  $J_H^{-/-}$  mice does not increase the number of PP M cells (our unpublished observations), indicating that the contribution of B cells to the development of M cells does not involve simply providing RANKL. Given that TNF family members are known to have overlapping and partially redundant functions in other developmental contexts (e.g. the known contributions of  $LT\alpha_1\beta_2$ , RANKL, and TNF- $\alpha$  to the normal formation and organization of secondary lymphoid structures) (44), other TNF family members may contribute to the induction of M cell differentiation and account for the low level of residual M cell formation in the absence of RANKL. Cooperation of RANKL with the TNF family member CD40L has recently been established for the induction of mTEC differentiation (24,25). RANKL is the most critical TNF family member in inducing normal mTEC differentiation during embryonic development of the thymus, with CD40L playing a complementary role in the postnatal thymus (24). Interesting parallels exist between the role of RANKL in inducing differentiation of UEA-I<sup>+</sup> M cells in the FAE of PP and its role in inducing the differentiation of UEA-I<sup>+</sup> mTEC in the thymus. The RANKL-induced mTECs are critical for establishment of central T cell tolerance, while RANKL-induced M cells contribute to the establishment of peripheral T cell tolerance to bacterial antigens at mucosal surfaces normally colonized by commensal bacteria.

The identification of RANKL as a key switch factor that can elicit M cell development by intestinal epithelial precursors has the potential to yield valuable translational applications in the areas of mucosal vaccine development and oral tolerance induction. Specifically targeting orally administered antigens to M cells using either monoclonal antibodies to M cell surface receptors, lectins, or bacterial adhesins specific for M cells remains an active area in the development of vaccines for oral delivery (45,46). Combining antibody-mediated M cell targeting of antigen with a strong mucosal adjuvant (e.g. cholera toxin) already shows promise as a strategy for the establishment of both mucosal and systemic immunity to vaccine antigens (47). The efficacy of such approaches may be boosted if preceded by systemic or ideally local delivery of exogenous RANKL aimed at increasing the frequency of human M cells in the PP FAE and particularly in the villous epithelium to supraphysiologic levels, thereby increasing the efficiency of delivery of M cell-targeted vaccines administered at mucosal surfaces.

## Supplementary Material

Refer to Web version on PubMed Central for supplementary material.

## Acknowledgments

We thank Dr. Max Cooper for valuable suggestions and Dr. Tim Denning for comments on the manuscript. We also thank Dr. Yongwon Choi for providing us with RANKL knockout mice, Katy Gray in Dr. Sam Speck's laboratory for help obtaining breeder pairs of  $\mu$ MT mice, and Jeannette Taylor from the Robert P. Apkarian Integrated Electron Microscopy Core for expert technical assistance with electron microscopy.

This work was supported by grants from the NIH (DK64730 to I.R.W. and DK64399 supporting the Imaging Core Facility of the Emory Digestive Diseases Research Development Center) and the Crohn's & Colitis Foundation of America (Senior Research Award to I.R.W.).

## References

1. Fagarasan S, Honjo T. Regulation of IgA synthesis at mucosal surfaces. *Curr. Opin. Immunol* 2004;16:277–283. [PubMed: 15134775]
2. Iweala OI, Nagler CR. Immune privilege in the gut: the establishment and maintenance of non-responsiveness to dietary antigens and commensal flora. *Immunol. Rev* 2006;213:82–100. [PubMed: 16972898]
3. Kraehenbuhl JP, Neutra MR. Epithelial M cells: differentiation and function. *Annu. Rev. Cell Dev. Biol* 2000;16:301–332. [PubMed: 11031239]
4. Pabst O, Bernhardt G, Forster R. The impact of cell-bound antigen transport on mucosal tolerance induction. *J. Leukoc. Biol* 2007;82:795–800. [PubMed: 17565048]
5. Martinoli C, Chiavelli A, Rescigno M. Entry route of *Salmonella typhimurium* directs the type of induced immune response. *Immunity* 2007;27:975–984. [PubMed: 18083577]
6. Hashizume T, Togawa A, Nochi T, Igarashi O, Kweon MN, Kiyono H, Yamamoto M. Peyer's patches are required for intestinal immunoglobulin A responses to *Salmonella*. *Infect. Immun* 2008;76:927–934.
7. Macpherson AJ, Uhr T. Compartmentalization of the mucosal immune responses to commensal intestinal bacteria. *Ann. N. Y. Acad. Sci* 2004;1029:36–43. [PubMed: 15681741]
8. Suzuki H, Sekine S, Kataoka K, Pascual DW, Maddaloni M, Kobayashi R, Fujihashi K, Kozono H, McGhee JR, Fujihashi K. Ovalbumin-protein sigma 1 M-cell targeting facilitates oral tolerance with reduction of antigen-specific CD4+ T cells. *Gastroenterology* 2008;135:917–925. [PubMed: 18565333]
9. Jang MH, Kweon MN, Iwatani K, Yamamoto M, Terahara K, Sasakawa C, Suzuki T, Nochi T, Yokota Y, Rennert PD, Hiroi T, Tamagawa H, Iijima H, Kunisawa J, Yuki Y, Kiyono H. Intestinal villous M cells: an antigen entry site in the mucosal epithelium. *Proc. Natl. Acad. Sci. U.S.A* 2004;101:6110–6115. [PubMed: 15071180]
10. Owen RL, Jones AL. Epithelial cell specialization within human Peyer's patches: an ultrastructural study of intestinal lymphoid follicles. *Gastroenterology* 1974;66:189–203. [PubMed: 4810912]
11. Kerneis S, Bogdanova A, Kraehenbuhl JP, Pringault E. Conversion by Peyer's patch lymphocytes of human enterocytes into M cells that transport bacteria. *Science* 1997;277:949–952. [PubMed: 9252325]
12. Mach J, Hshieh T, Hsieh D, Grubbs N, Chervonsky A. Development of intestinal M cells. *Immunol. Rev* 2005;206:177–189. [PubMed: 16048549]
13. Kerneis S, Pringault E. Plasticity of the gastrointestinal epithelium: the M cell paradigm and opportunism of pathogenic microorganisms. *Semin. Immunol* 1999;11:205–215. [PubMed: 10381866]
14. Gebert A, Fassbender S, Werner K, Weissferdt A. The development of M cells in Peyer's patches is restricted to specialized dome-associated crypts. *Am. J. Pathol* 1999;154:1573–1582. [PubMed: 10329609]
15. Lelouard H, Sahuquet A, Reggio H, Montcourrier P. Rabbit M cells and dome enterocytes are distinct cell lineages. *Journal of cell science* 2001;114:2077–2083. [PubMed: 11493643]
16. Bachmann MF, Wong BR, Josien R, Steinman RM, Oxenius A, Choi Y. TRANCE, a tumor necrosis factor family member critical for CD40 ligand-independent T helper cell activation. *J. Exp. Med* 1999;189:1025–1031. [PubMed: 10190893]
17. Lum L, Wong BR, Josien R, Becherer JD, Erdjument-Bromage H, Schlondorff J, Tempst P, Choi Y, Blobel CP. Evidence for a role of a tumor necrosis factor- $\alpha$  (TNF- $\alpha$ )-converting enzyme-like protease in shedding of TRANCE, a TNF family member involved in osteoclastogenesis and dendritic cell survival. *J. Biol. Chem* 1999;274:13613–13618. [PubMed: 10224132]
18. Hikita A, Yana I, Wakeyama H, Nakamura M, Kadono Y, Oshima Y, Nakamura K, Seiki M, Tanaka S. Negative regulation of osteoclastogenesis by ectodomain shedding of receptor activator of NF- $\kappa$ B ligand. *J. Biol. Chem* 2006;281:36846–36855. [PubMed: 17018528]
19. Wong BR, Josien R, Lee SY, Vologodskaya M, Steinman RM, Choi Y. The TRAF family of signal transducers mediates NF- $\kappa$ B activation by the TRANCE receptor. *J. Biol. Chem* 1998;273:28355–28359. [PubMed: 9774460]

20. Galibert L, Tometsko ME, Anderson DM, Cosman D, Dougall WC. The involvement of multiple tumor necrosis factor receptor (TNFR)-associated factors in the signaling mechanisms of receptor activator of NF- $\kappa$ B, a member of the TNFR superfamily. *J. Biol. Chem* 1998;273:34120–34127. [PubMed: 9852070]
21. Simonet WS, Lacey DL, Dunstan CR, Kelley M, Chang MS, Luthy R, Nguyen HQ, Wooden S, Bennett L, Boone T, Shimamoto G, DeRose M, Elliott R, Colombero A, Tan HL, Trail G, Sullivan J, Davy E, Bucay N, Renshaw-Gegg L, Hughes TM, Hill D, Pattison W, Campbell P, Sander S, Van G, Tarpley J, Derby P, Lee R, Boyle WJ. Osteoprotegerin: a novel secreted protein involved in the regulation of bone density. *Cell* 1997;89:309–319. [PubMed: 9108485]
22. Kong YY, Yoshida H, Sarosi I, Tan HL, Timms E, Capparelli C, Morony S, Oliveira-dos-Santos AJ, Van G, Itie A, Khoo W, Wakeham A, Dunstan CR, Lacey DL, Mak TW, Boyle WJ, Penninger JM. OPGL is a key regulator of osteoclastogenesis, lymphocyte development and lymph-node organogenesis. *Nature* 1999;397:315–323. [PubMed: 9950424]
23. Kim N, Odgren PR, Kim DK, Marks SC Jr, Choi Y. Diverse roles of the tumor necrosis factor family member TRANCE in skeletal physiology revealed by TRANCE deficiency and partial rescue by a lymphocyte-expressed TRANCE transgene. *Proc. Natl. Acad. Sci. U.S.A* 2000;97:10905–10910. [PubMed: 10984520]
24. Akiyama T, Shimo Y, Yanai H, Qin J, Ohshima D, Maruyama Y, Asaumi Y, Kitazawa J, Takayanagi H, Penninger JM, Matsumoto M, Nitta T, Takahama Y, Inoue J. The tumor necrosis factor family receptors RANK and CD40 cooperatively establish the thymic medullary microenvironment and self-tolerance. *Immunity* 2008;29:423–437. [PubMed: 18799149]
25. Hikosaka Y, Nitta T, Ohigashi I, Yano K, Ishimaru N, Hayashi Y, Matsumoto M, Matsuo K, Penninger JM, Takayanagi H, Yokota Y, Yamada H, Yoshikai Y, Inoue J, Akiyama T, Takahama Y. The cytokine RANKL produced by positively selected thymocytes fosters medullary thymic epithelial cells that express autoimmune regulator. *Immunity* 2008;29:438–450. [PubMed: 18799150]
26. Wong BR, Josien R, Lee SY, Sauter B, Li HL, Steinman RM, Choi Y. TRANCE (tumor necrosis factor [TNF]-related activation-induced cytokine), a new TNF family member predominantly expressed in T cells, is a dendritic cell-specific survival factor. *J. Exp. Med* 1997;186:2075–2080. [PubMed: 9396779]
27. Fata JE, Kong YY, Li J, Sasaki T, Irie-Sasaki J, Moorehead RA, Elliott R, Scully S, Voura EB, Lacey DL, Boyle WJ, Khokha R, Penninger JM. The osteoclast differentiation factor osteoprotegerin-ligand is essential for mammary gland development. *Cell* 2000;103:41–50. [PubMed: 11051546]
28. Yoshida H, Naito A, Inoue J, Satoh M, Santee-Cooper SM, Ware CF, Togawa A, Nishikawa S. Different cytokines induce surface lymphotoxin- $\alpha\beta$  on IL-7 receptor- $\alpha$  cells that differentially engender lymph nodes and Peyer's patches. *Immunity* 2002;17:823–833. [PubMed: 12479827]
29. Taylor RT, Patel SR, Lin E, Butler BR, Lake JG, Newberry RD, Williams IR. Lymphotoxin-independent expression of TNF-related activation-induced cytokine by stromal cells in cryptopatches, isolated lymphoid follicles, and Peyer's patches. *J. Immunol* 2007;178:5659–5667. [PubMed: 17442949]
30. Katakai T, Suto H, Sugai M, Gonda H, Togawa A, Suematsu S, Ebisuno Y, Katagiri K, Kinashi T, Shimizu A. Organizer-like reticular stromal cell layer common to adult secondary lymphoid organs. *J. Immunol* 2008;181:6189–6200. [PubMed: 18941209]
31. Kim D, Mebius RE, MacMicking JD, Jung S, Cupedo T, Castellanos Y, Rho J, Wong BR, Josien R, Kim N, Rennert PD, Choi Y. Regulation of peripheral lymph node genesis by the tumor necrosis factor family member TRANCE. *J. Exp. Med* 2000;192:1467–1478. [PubMed: 11085748]
32. Kubota K, Sakikawa C, Katsumata M, Nakamura T, Wakabayashi K. Platelet-derived growth factor BB secreted from osteoclasts acts as an osteoblastogenesis inhibitory factor. *J. Bone Miner. Res* 2002;17:257–265. [PubMed: 11811556]
33. Pappo J, Ermak TH. Uptake and translocation of fluorescent latex particles by rabbit Peyer's patch follicle epithelium: a quantitative model for M cell uptake. *Clin. Exp. Immunol* 1989;76:144–148. [PubMed: 2661061]



34. Chabot S, Wagner JS, Farrant S, Neutra MR. TLRs regulate the gatekeeping functions of the intestinal follicle-associated epithelium. *J. Immunol* 2006;176:4275–4283. [PubMed: 16547265]
35. Terahara K, Yoshida M, Igarashi O, Nochi T, Pontes GS, Hase K, Ohno H, Kurokawa S, Mejima M, Takayama N, Yuki Y, Lowe AW, Kiyono H. Comprehensive gene expression profiling of Peyer's patch M cells, villous M-like cells, and intestinal epithelial cells. *J. Immunol* 2008;180:7840–7846. [PubMed: 18523247]
36. Kamijo S, Nakajima A, Ikeda K, Aoki K, Ohya K, Akiba H, Yagita H, Okumura K. Amelioration of bone loss in collagen-induced arthritis by neutralizing anti-RANKL monoclonal antibody. *Biochem. Biophys. Res. Commun* 2006;347:124–132. [PubMed: 16815304]
37. Golovkina TV, Shlomchik M, Hannum L, Chervonsky A. Organogenic role of B lymphocytes in mucosal immunity. *Science* 1999;286:1965–1968. [PubMed: 10583962]
38. Luger A, Floer M, Westphal S, Maaser C, Spahn TW, Schmidt MA, Domschke W, Williams IR, Kucharzik T. Absence of CCR6 inhibits CD4+ regulatory T-cell development and M-cell formation inside Peyer's patches. *Am. J. Pathol* 2005;166:1647–1654. [PubMed: 15920150]
39. Neutra MR, Mantis NJ, Kraehenbuhl JP. Collaboration of epithelial cells with organized mucosal lymphoid tissues. *Nat. Immunol* 2001;2:1004–1009. [PubMed: 11685223]
40. Kunisawa J, Nochi T, Kiyono H. Immunological commonalities and distinctions between airway and digestive immunity. *Trends Immunol* 2008;29:505–513. [PubMed: 18835748]
41. des Rieux A, Fievez V, Theate I, Mast J, Preat V, Schneider YJ. An improved in vitro model of human intestinal follicle-associated epithelium to study nanoparticle transport by M cells. *Eur. J. Pharm. Sci* 2007;30:380–391. [PubMed: 17291730]
42. Williamson E, Bilsborough JM, Viney JL. Regulation of mucosal dendritic cell function by receptor activator of NF- $\kappa$ B (RANK)/RANK ligand interactions: impact on tolerance induction. *J. Immunol* 2002;169:3606–3612. [PubMed: 12244151]
43. Totsuka T, Kanai T, Nemoto Y, Tomita T, Okamoto R, Tsuchiya K, Nakamura T, Sakamoto N, Akiba H, Okumura K, Yagita H, Watanabe M. RANK-RANKL signaling pathway is critically involved in the function of CD4+CD25+ regulatory T cells in chronic colitis. *J. Immunol* 2009;182:6079–6087. [PubMed: 19414759]
44. Pfeffer K. Biological functions of tumor necrosis factor cytokines and their receptors. *Cytokine Growth Factor Rev* 2003;14:185–191. [PubMed: 12787558]
45. Foxwell AR, Cripps AW, Kyd JM. Optimization of oral immunization through receptor-mediated targeting of M cells. *Hum. Vaccin* 2007;3:220–223. [PubMed: 17643069]
46. Chionh YT, Wee JL, Every AL, Ng GZ, Sutton P. M-cell targeting of whole killed bacteria induces protective immunity against gastrointestinal pathogens. *Infect. Immun* 2009;77:2962–2970. [PubMed: 19380476]
47. Nochi T, Yuki Y, Matsumura A, Mejima M, Terahara K, Kim DY, Fukuyama S, Iwatsuki-Horimoto K, Kawaoka Y, Kohda T, Kozaki S, Igarashi O, Kiyono H. A novel M cell-specific carbohydrate-targeted mucosal vaccine effectively induces antigen-specific immune responses. *J. Exp. Med* 2007;204:2789–2796. [PubMed: 17984304]

## Abbreviations used in this paper

FAE	follicle-associated epithelium
PP	Peyer's patch
ILF	isolated lymphoid follicle
RANKL	receptor activator of NF- $\kappa$ B ligand
RANK	receptor activator of NF- $\kappa$ B
DC	dendritic cell
UEA-I	<i>Ulex europaeus</i> agglutinin-I
mTEC	medullary thymic epithelial cells

LT	lymphotoxin
DAPI	4',6-diamidino-2-phenylindole

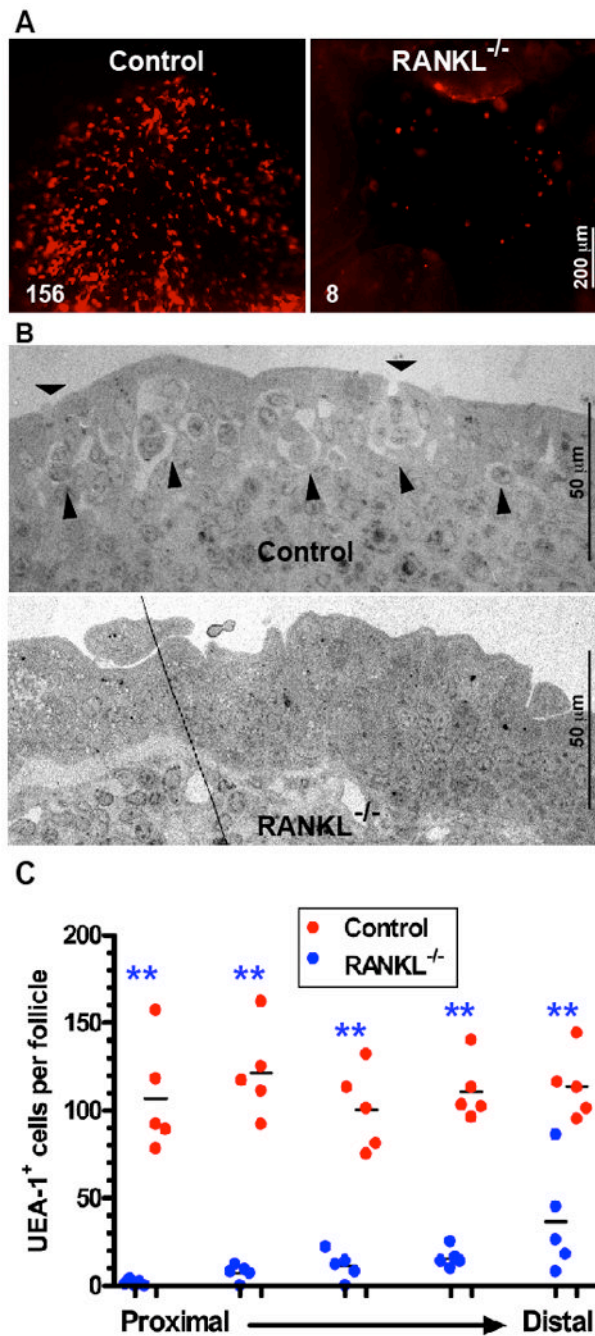


**Figure 1.**

PP of RANKL null mice contain very few M cells. A, UEA-I staining reveals far fewer M cells in a representative follicle from a PP from a (C57BL/6 X BALB/c)<sub>F1</sub> RANKL null compared to a wild type control PP. The number of M cells counted in the follicle is indicated in the lower left hand corner. The follicles shown are from the middle portion of the small intestine. Scale bar, 200 μm. B, FAE from (C57BL/6 X BALB/c)<sub>F1</sub> RANKL null mice showed a lack of characteristic M cell features by transmission electron microscopy. The long arrowheads indicate intraepithelial pockets within the M cells of wild type FAE. The short arrowheads point to the shorter microvilli found on the apical surface of M cells. Scale bars, 50 μm. C, Scatter plot summarizing frequency of UEA-I<sup>+</sup> M cells in individual

PP follicles from mixed background RANKL null and control mice (n=5 mice for both groups). All PP examined were assigned to 1 of 5 groups based on proximal to distal position. \*\*,  $p \leq 0.001$  compared to control mice by ANOVA.

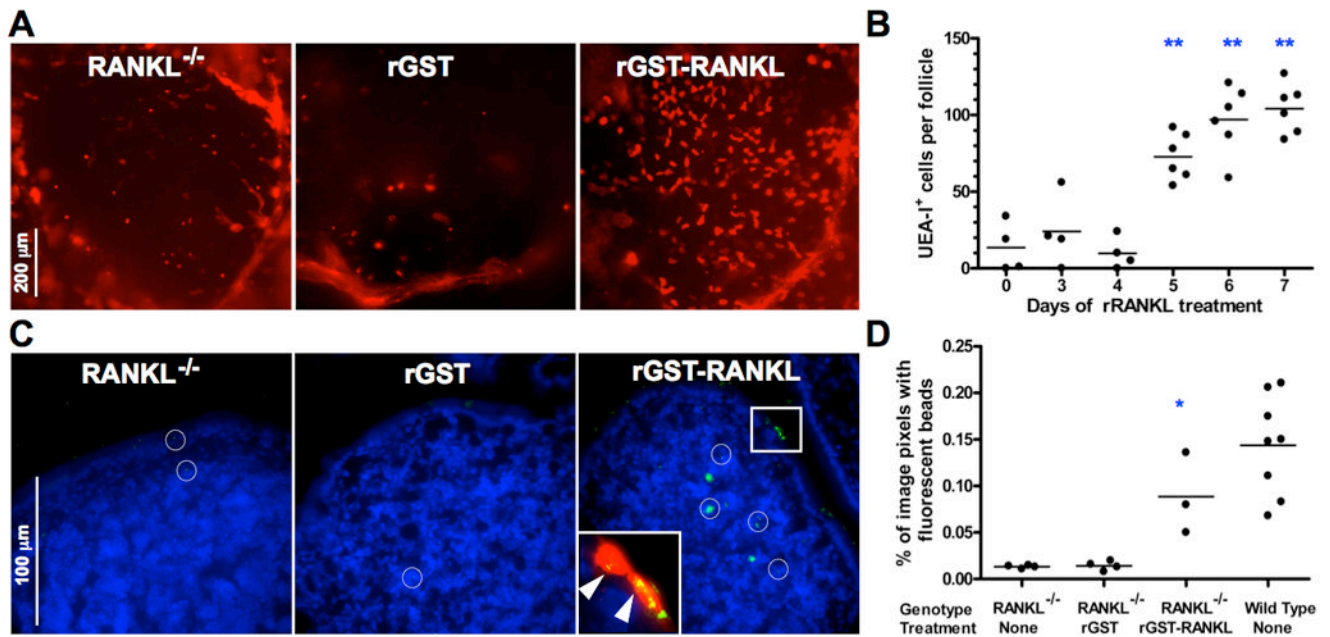


**Figure 2.**

Administration of rRANKL to RANKL null mice restores PP M cells. A, (C57BL/6 X BALB/c)<sub>F1</sub> RANKL null mice were treated i.p. for 7 days with 250  $\mu$ g/day of GST-RANKL or GST as a control. UEA-I staining of representative follicles from the distal small intestine shows restoration of the normal number and pattern of UEA-I<sup>+</sup> M cells by GST-RANKL, but not by GST. Scale bar, 200  $\mu$ m. B, Reconstitution of UEA-I<sup>+</sup> M cells requires 5 days of treatment with GST-RANKL. The results are based on 3 to 6 mixed background mice at each time point and include data from all PP except the most distal PP. \*\* indicates  $p \leq 0.001$  compared to untreated mice by ANOVA. C, Uptake of 200 nm diameter fluorescent beads from isolated small intestinal loops into PP of mixed background RANKL null mice 90 minutes after bead injection is restored to near wild type levels by prior treatment with GST-RANKL for 5 days. Merged images of bead fluorescence and DAPI fluorescence from frozen sections of PP are shown with the white circles indicating the location of individual beads or clusters of beads. The inset shows a magnified image of the boxed area additionally merged with the rhodamine-UEA-I signal to show that the clusters of fluorescent beads (indicated by arrowheads) within 2 adjacent UEA-I<sup>+</sup> M cells on the surface of the FAE. Scale bar, 100  $\mu$ m. D, Summary scatter plot showing that GST-RANKL treatment reconstitutes uptake of fluorescent beads as assessed by image analysis of the percentage of pixels containing green fluorescent beads within the area of the PP follicles. \*,  $p < 0.01$  compared to untreated RANKL null mice by ANOVA.



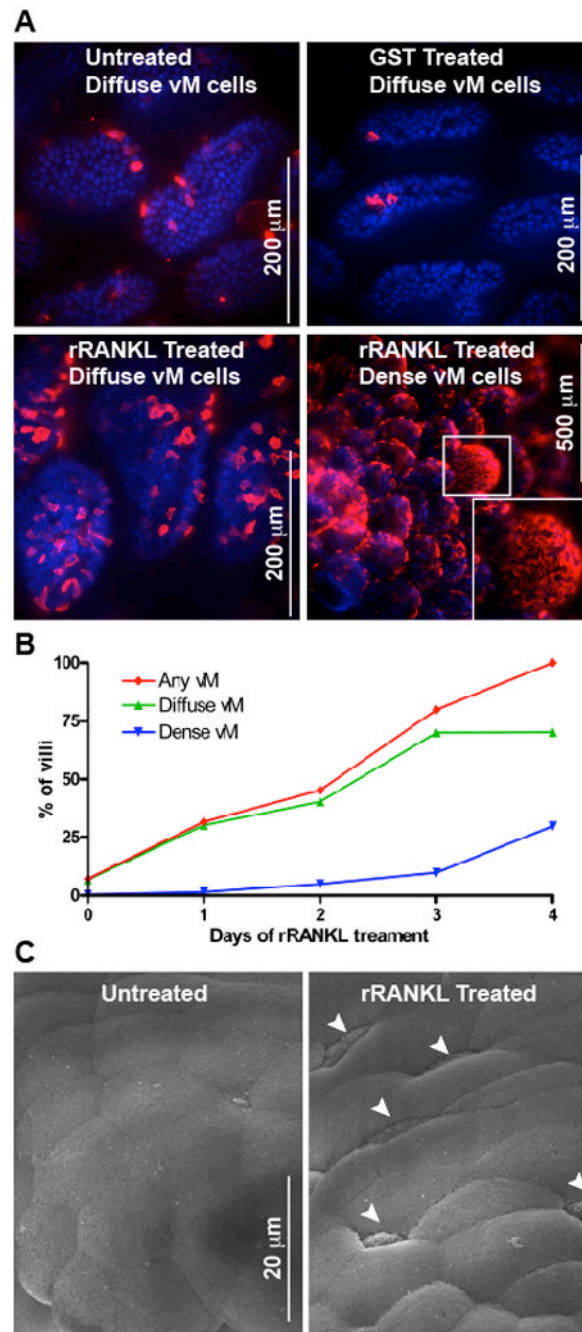


**Figure 3.**

Administration of rRANKL induces development of villous M cells on all small intestinal villi. A, Whole mount staining of villous M cells in untreated BALB/c mice and mice treated for 4 days with GST-RANKL or GST (an initial injection of 50  $\mu$ g i.p. followed by 100  $\mu$ g s.c. every 24 h) with rhodamine-UEA-I and DAPI. In untreated mice, a few villous M cells in a diffuse pattern are present on occasional villi. GST-RANKL treatment leads to an increased fraction of the villi having M cells and an increase in the number of M cells per villus. The fraction of villi exhibiting both the diffuse and dense patterns of villous M cell distribution increases after GST-RANKL. Scale bars, 200  $\mu$ m and 500  $\mu$ m. B, Summary graph showing kinetics of induction of villous M cells in the diffuse and dense patterns of

distribution following GST-RANKL administration. C, Scanning electron microscopy reveals the presence of cells with a depressed surface and attenuated and blunted microvilli characteristic of M cells.

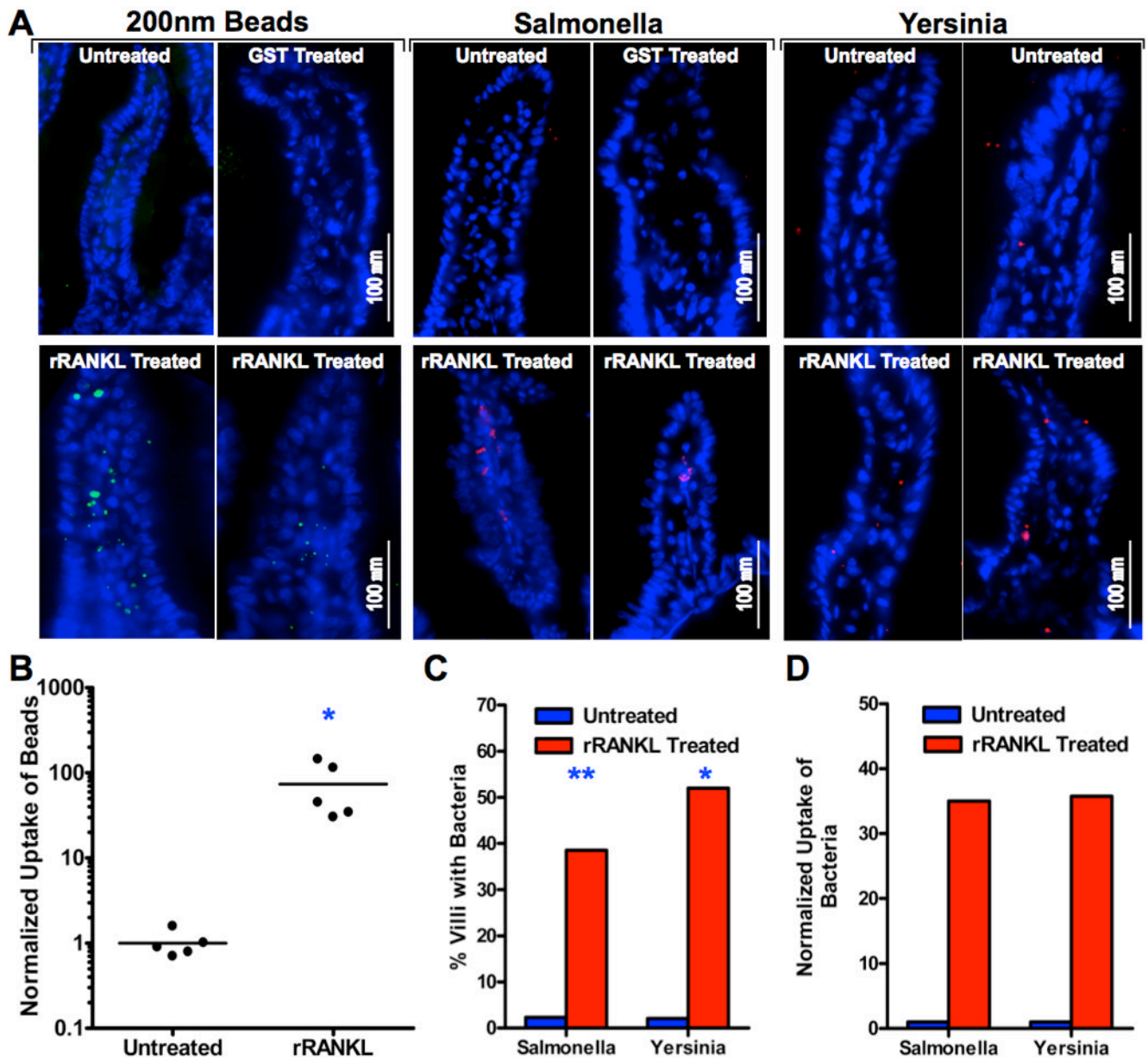


**Figure 4.**

RANKL-induced villous M cells are functional for bead and bacteria uptake from the intestinal lumen. A, Wild type (C57BL/6 X BALB/c) $F_1$  mice were treated with 100  $\mu$ g of GST-RANKL or GST s.c. once a day for 4 consecutive days. On the last two days of injections, the mice and untreated controls also received  $1 \times 10^{11}$  200 nm fluorescent beads by gavage. One day after the last dose of GST-RANKL or GST, segments of small intestine were harvested and sectioned to check for the presence of green fluorescent beads. Alternatively, isolated small intestinal loops were prepared in anesthetized mice treated for 4 days with RANKL or GST and untreated controls and these loops were injected with paraformaldehyde-fixed *Salmonella enterica* serovar Typhimurium expressing DsRed-Express or *Yersinia enterocolitica* labeled with Alexa546. After a 2 h incubation, the tissue was harvested for frozen sections. The merged images show representative villi with DAPI positive nuclei and either green fluorescent beads or red fluorescent bacteria within the villi.

B, Uptake of beads was quantitated by image analysis and normalized so that the average uptake in untreated controls was 1.0. \*,  $p < 0.01$  by Mann-Whitney test. C, The percentage of villi containing at least one bacterial organism was substantially increased in RANKL-treated mice. \*\*,  $p \leq 0.001$ ; \*,  $p < 0.01$  (both by Fisher's exact test). D, Uptake of bacteria was quantitated by counting individual bacteria within villi. The mean number of bacteria found per villus was normalized to a value of 1.0 for the untreated controls.

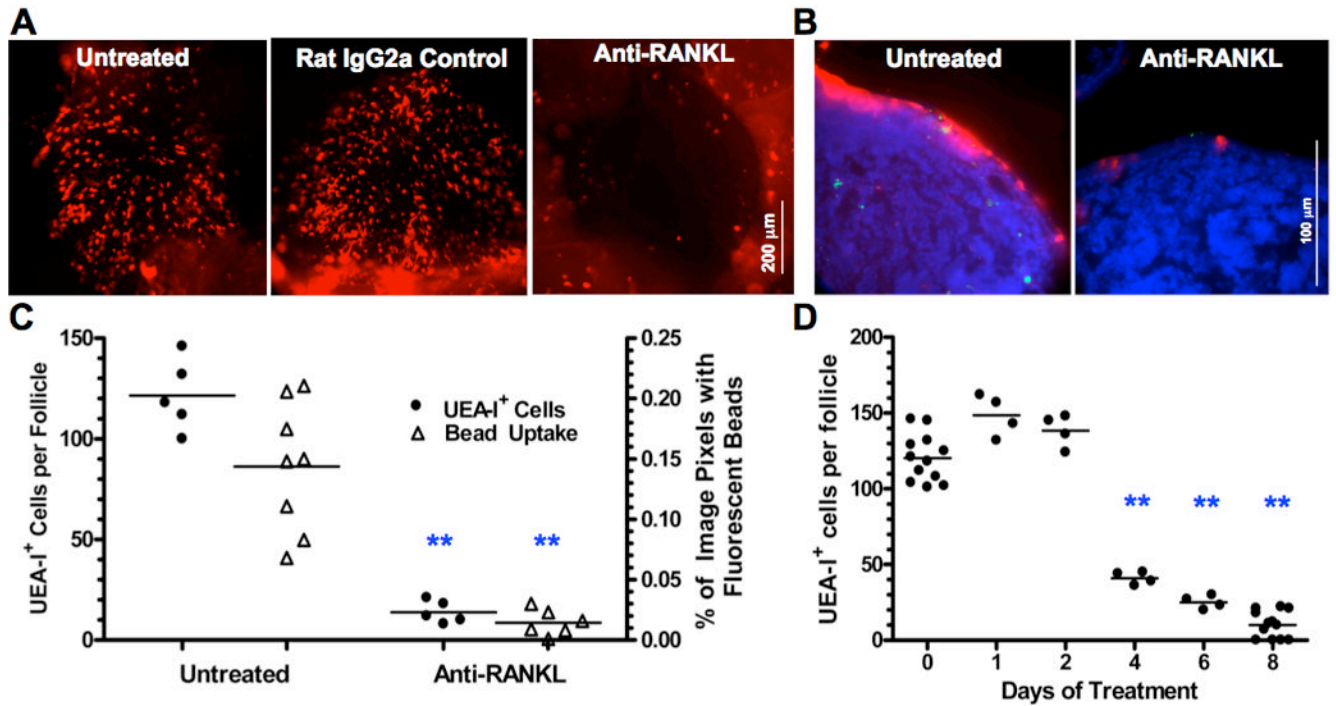


**Figure 5.**

Treatment of wild type mice with neutralizing anti-RANKL leads to loss of PP M cells. A,B, BALB/c mice were treated i.p. with 250  $\mu$ g of IKK22-5 mAb or an isotype control rat IgG2a mAb on days 0, 2, 4, and 6. On day 8, isolated bowel loops containing PP were injected with fluorescent beads and the mice euthanized after 90 minutes. Anti-RANKL treatment led to loss of UEA-I<sup>+</sup> M cells detected by whole mount staining (A) and a decrease in the uptake of fluorescent beads detected on frozen sections of PP from the bead-injected loops (B).

Scale bar, 200  $\mu$ m in A and 100  $\mu$ m in B. C, Summary of data from all PP analyzed in A and B for UEA-I<sup>+</sup> cells and fluorescent bead uptake. D, Anti-RANKL-induced loss of UEA-I<sup>+</sup> M cells detected by whole mount staining begins by 4 days after start of antibody treatment.

\*\* in C and D indicates  $p < 0.001$  compared to untreated mice by t-test (C) or ANOVA (D).



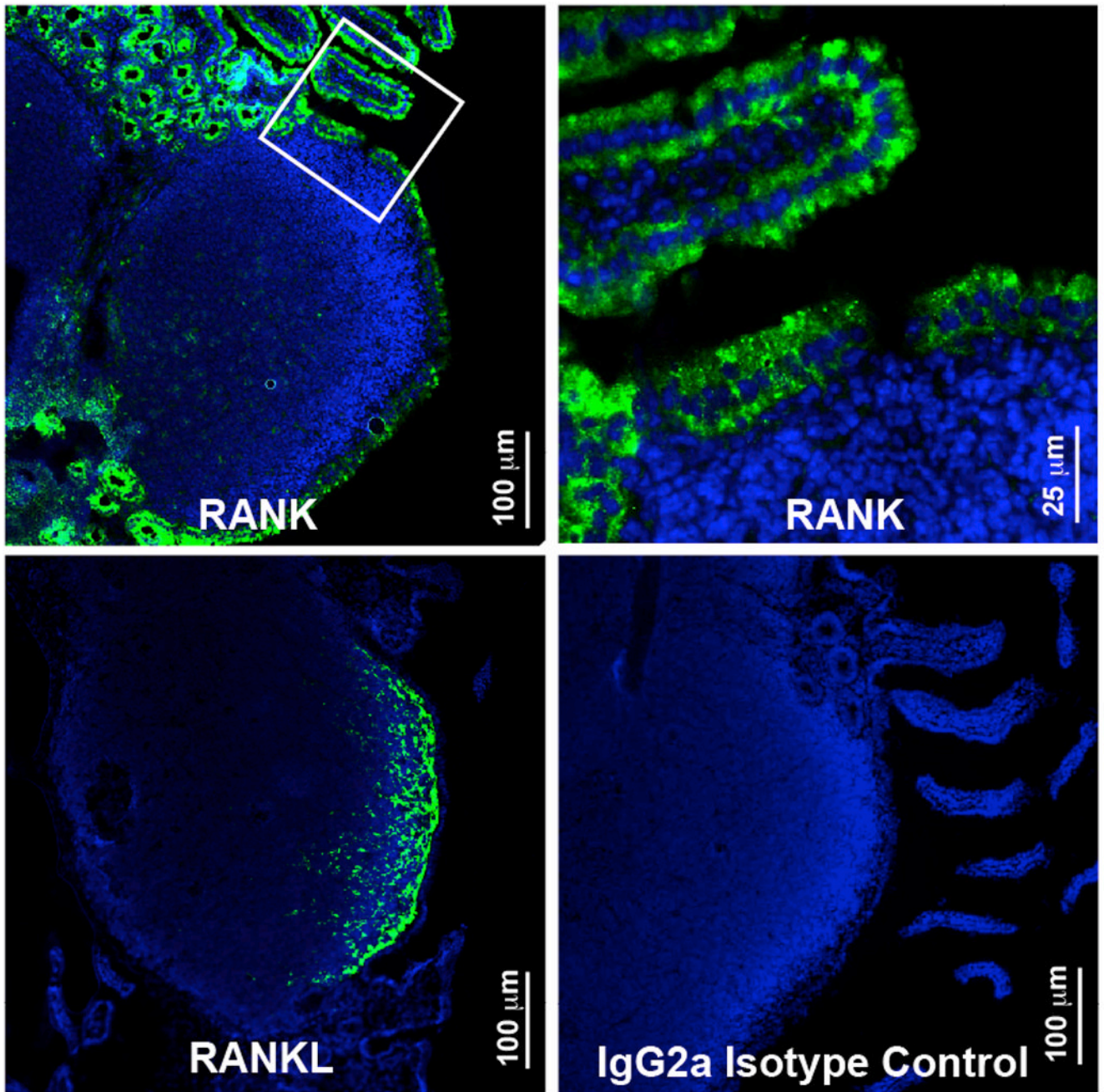


**Figure 6.**

Intestinal epithelial cells express RANK. Frozen sections of a PP from a single wild type BALB/c mouse were stained with rat mAbs to mouse RANK (A, B), mouse RANKL (C), or an isotype control rat IgG2a mAb (D), followed by a biotinylated secondary antibody, streptavidin-peroxidase, and FITC-tyramide plus DAPI as a counterstain. A, RANK expression is localized to epithelial cells in the FAE and on the adjacent villi. Scale bar, 100 μm. B, Higher magnification of boxed area from A showing that RANK is present on both the apical and basolateral surfaces of the FAE. Scale bar, 250 μm. C, Reticular stromal cells concentrated immediately beneath the epithelial layer are the only cells on which RANKL is detected. Scale bar, 200 μm. D, No staining is observed with the rat IgG2a isotype control.

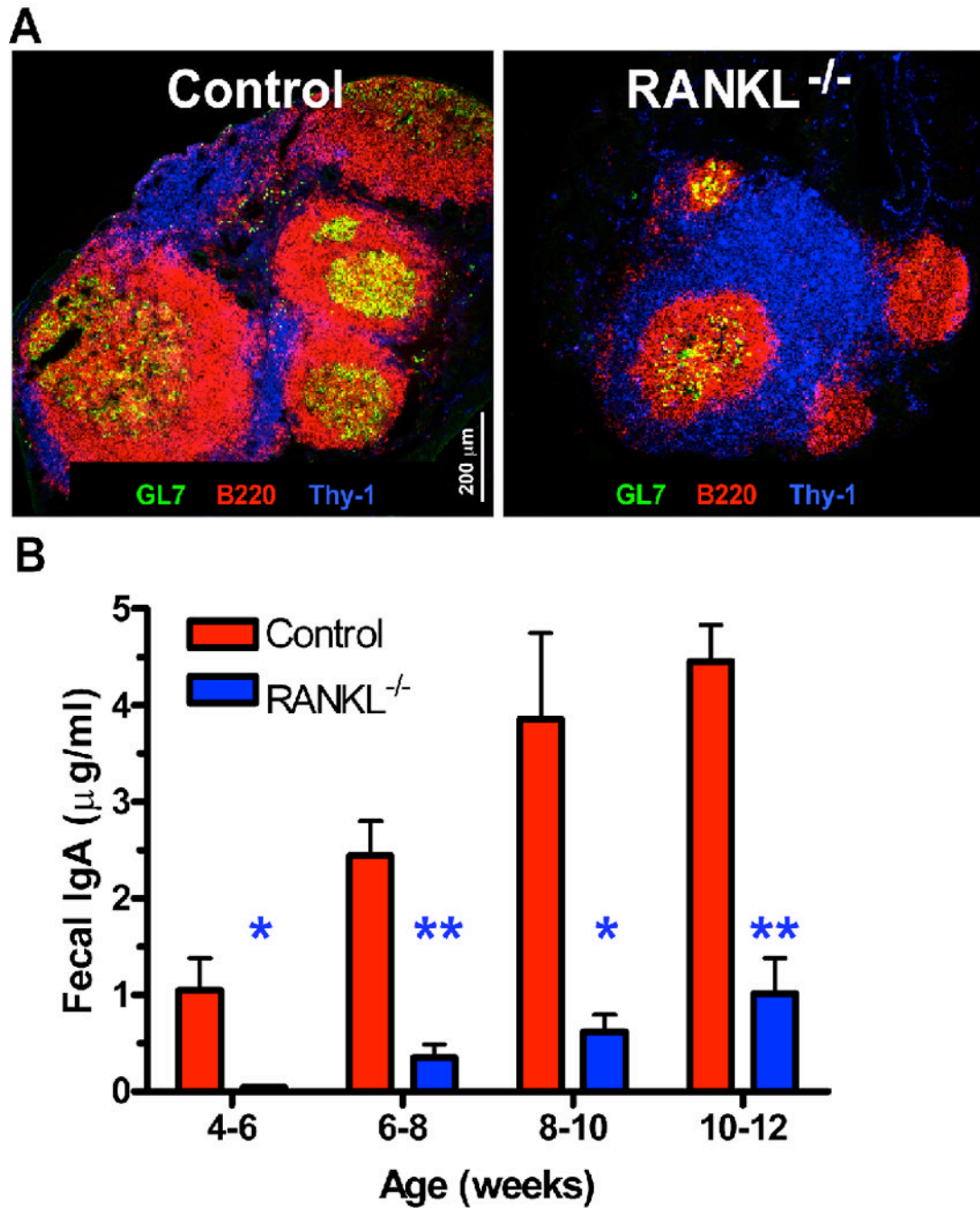


**Figure 7.** RANKL<sup>-/-</sup> mice have fewer germinal centers in their PP follicles and lower levels of fecal IgA. A, RANKL<sup>-/-</sup> PP on a mixed C57BL/6 and BALB/c background have fewer and less developed germinal centers identified by GL7<sup>+</sup> cells than control PP. B, Fecal IgA concentrations (mean ± S.D.) measured by ELISA were consistently decreased in RANKL<sup>-/-</sup> mice compared to littermate controls based on analysis of samples from 5 to 16 mice of each genotype in each age range tested. \*, p < 0.01; \*\*, p < 0.001 (compared to control mice by t-test).